Combust. Sci. and Tech., 1995, Vol. 108, pp. 363–382
Reprints available directly from the publisher
Photocopying permitted by license only

© 1995 OPA (Overseas Publishers Association)
Amsterdam B.V. Published in The Netherlands
under license by Gordon and Breach Science
Publishers SA
Printed in Malaysia

Mathematical Modelling of NO Formation in a Power Station Boiler

P. J. COELHO and M. G. CARVALHO *Instituto Superior Técnico, Mechanical Engineering Department, Technical University of Lisbon, Av. Rovisco Pais, 1096 Lisboa Codex, Portugal*

(Received June 21, 1995)

ABSTRACT—This paper reports the application of a full three-dimensional mathematical model to a fuel-oil fired power station boiler of the Portuguese Electricity Utility. Special emphasis is placed on the formation of nitric oxide. Models for thermal and fuel-NO formation are included and several variants of the models are employed. The predicted results are compared with measurements. Concentrations of O_2, CO_2 and CO are in good agreement with the data whereas the temperature, although in qualitative agreement, is underestimated along the profile crossing the flame region. It is shown that fuel NO is an important source of the total NO formed. Nevertheless, the NO mole fraction is underestimated. Several hypotheses were checked to identify the source of discrepancy and the most probable ones are the temperature underestimation in the flame region and the experimental uncertainties.

Key Words: Combustion in practical systems-furnaces, environmental combustion-NO_x

INTRODUCTION

The environmental impact of pollutants emissions from power station boilers has received increased attention. The harmful effects of such emissions on living beings motivated the governments to fix by legislation the maxima levels of emissions. The problem is enhanced by the tendency to burn alternative fuels which, in general, are of poor quality yielding more pollutants. To face these constrainments modifications in boilers operation or in burner equipment are often needed. The investigation of such modifications and the search for low emission burners are key issues at present. Mathematical models provide a valuable help in these investigations.

Several studies using full three-dimensional mathematical models have been published during the last years (see, e.g., Robinson, 1985; Abbas and Lockwood, 1986; Boyd and Kent, 1986; Görner and Zinser, 1988; Fiveland and Wessel, 1988; Carvalho and Coelho, 1990). However, the problem of modelling NO formation in utility boilers has only recently been addressed. Carvalho *et al.* (1991), Bonvini *et al.* (1991) and De Michele *et al.* (1991) calculated thermal NO formation in gas and oil-fired boilers. In the first two works the model was based on the Zeldovich mechanism and the last work employed a more complex reaction scheme based on 27 chemical reactions and 17 species. There seems to be little justification to employ such a complex scheme since turbulent fluctuations cannot be considered and, therefore, the improvement of solution accuracy is doubtful. The calculation of NO formation in coal-fired boilers has been presented by Fiveland *et al.* (1987), Fiveland and Wessel (1991), Epple and Schnell

(1992) and Coimbra *et al.* (1994). They model fuel-NO formation assuming that HCN acts as an intermediate of fuel-NO. The formation of fuel-NO results from the oxidation of HCN and the reduction of fuel-NO occurs when HCN reacts with NO. Fuel-NO can also be reduced by heterogeneous reaction with the char. In addition, thermal NO is modelled using the Zeldovich mechanism.

The present work is an extension of the preliminary study reported in Carvalho *et al.* (1991). It describes the application of a mathematical model to a boiler of the Portuguese Electricity Utility with special emphasis placed on the NO formation. In addition to the thermal-NO formation model, a fuel-NO formation model was also included. Several variants of both models were employed. Prompt-NO was neglected since its contribution to the total NO formed in utility boilers is very small. The results are compared with recent measurements acquired in the boiler by Cassiano *et al.* (1994).

The mathematical model is described in the next section with emphasis on the NO formation models. Then, the results are presented and discussed, after a brief description of the boiler. The main conclusions are drawn in the last section.

MATHEMATICAL MODEL

Governing Equations and Physical Submodels

The mathematical model is based on the solution of the density weighted average form of the conversation equations for mass, momentum and energy and transport equations for scalar quantities. The equations are closed using the k-ε turbulence model. Combustion is modelled using the conserved scalar/prescribed probability density function (p.d.f.) formulation. A clipped Gaussian p.d.f. was used. Chemical equilibrium is assumed to relate instantaneous mass fractions and temperature with the conserved scalar, taken as the mixture fraction. Radiation is calculated using the discrete transfer method. The absorption coefficient of the medium is obtained using the two gray plus one clear gas approach extended to account for soot. A simple model of soot formation and oxidation in incorporated to estimate its concentration. The discretized equations are solved using a finitie volume/finite difference method. Details of the mathematical model may be found, e.g., in Carvalho *et al.* (1987).

Computation of nitric oxide distribution is decoupled from the model outlined above since its concentration is too small to influence significantly the temperature field and the major gas species concentrations. Hence, the results of the previous model are used in a post-processor to predict NO concentration. The post-processor is based on the solution of transport equations for NO and HCN. The source terms of these equations are computed using the models described below.

Thermal NO Formation Model

Fundamentals Thermal NO is formed from atmospheric nitrogen according to the extended Zeldovich mechanism that comprises the following steps:

$$O + N_2 \rightleftarrows NO + N \tag{1}$$

$$N + O_2 \rightleftarrows NO + O \tag{2}$$

$$N + OH \rightleftarrows NO + H \tag{3}$$

The steady state approximation for the nitrogen atom concentration yields:

$$\frac{d[NO]}{dt} = \frac{2k_1[O][N_2]}{1 + \dfrac{k_{-1}[NO]}{k_2[O_2] + k_3[OH]}} \cdot \left(1 - \frac{k_{-1}[NO]}{k_2[O_2] + k_3[OH]}\left(\frac{k_{-2}[NO]}{k_1[N_2]} + \frac{k_{-3}[NO][H]}{k_3[O][N_2]}\right)\right) \tag{4}$$

where k_1, k_2, k_3, k_{-1}, k_{-2} and k_{-3} are the forward and reverse rate constants of reactions 1, 2 and 3, respectively. Assuming that the reaction:

$$O + OH \rightleftarrows O_2 + H \tag{5}$$

is in partial equilibrium, we have:

$$[H] = \frac{k_{-2}k_3}{k_2 k_{-3}} \frac{[O][OH]}{[O_2]} \tag{6}$$

Substitution of this relation in Eq. (4) yields:

$$\frac{d[NO]}{dt} = \frac{2k_1[O][N_2]}{1 + \dfrac{k_{-1}[NO]}{k_2[O_2] + k_3[OH]}} \left(1 - \frac{k_{-1}k_{-2}}{k_1 k_2} \frac{[NO]^2}{[N_2][O_2]}\right) \tag{7}$$

This expression may be simplified when the [OH] concentration is very small, as in most lean flames. Hence, neglecting reaction (3):

$$\frac{d[NO]}{dt} = \frac{2[O](k_1 k_2[O_2][N_2] - k_{-1}k_{-2}[NO]^2)}{k_2[O_2] + k_{-1}[NO]} \tag{8}$$

If [NO] concentration is very small or the reverse reactions are negligible a further simplification is possible:

$$\frac{d[NO]}{dt} = 2k_1[O][N_2] \tag{9}$$

As recognized by Dupont *et al.* (1993), the difficulty in modelling thermal NO is not the lack of knowledge of the chemical mechanism but the problem of applying it with precision. They state that thermal NO can be modelled with an accuracy of $\pm 35\%$ if the actual [O] an [OH] concentrations are used rather than the equilibrium values. Unfortunately, only [O] and [OH] equilibrium concentrations can be obtained from the combustion model employed in the present work. This problem has also been experienced by all the authors mentioned in the introduction who studied NO formation in utility boilers, except De Michele *et al.* (1991) who neglected turbulent fluctuations. To estimate [O] and [OH] concentrations we employed four different approaches.

Model 1 The first model assumes partial equilibrium of the reaction:

$$O_2 + M \rightleftarrows O + O + M \tag{10}$$

where M is an inert radical. Hence, we have:

$$[O] = \left(\frac{k_{10}}{k_{-10}}[O_2]\right)^{1/2} \tag{11}$$

The concentration of [OH] was neglected and Eq. (8) was used to calculate the rate of thermal NO formation. Previous works in utility boilers mentioned in the introduction generally follow this approach, but they often neglect also the reverse reactions and employ Eq. (9) instead of Eq. (8).

Model 2 In the flame regions where hydrocarbons are consumed, oxygen concentration often significantly exceeds the levels predicted by Eq. (11). In such regions, partial equilibrium of the following reactions was assumed (see, e.g. Iverach *et al.*, 1973; Boardman, 1990):

$$H_2 + O_2 \rightleftarrows OH + O \tag{12}$$

$$CO + OH \rightleftarrows CO_2 + H \tag{13}$$

yielding:

$$[O] = \frac{k_{12}k_{13}}{k_{-12}k_{-13}}\frac{[O_2][CO]}{[CO_2]} \tag{14}$$

This expression was only used in fuel rich regions and expression (11) was employed elsewhere. [OH] concentration was neglected again and equation (8) was used to calculate the rate of formation of thermal NO.

Model 3 This model is based on the assumption of partial equilibrium of the chain-branching and propagation reactions of the hydrogen-oxygen mechanism (see Schott, 1960; Warnatz, 1992):

$$OH + H_2 \rightleftarrows H_2O + H \tag{15}$$

$$H + O_2 \rightleftarrows OH + O \tag{16}$$

$$O + H_2 \rightleftarrows OH + H \tag{17}$$

This allows the calculation of [H], [O] and [OH] in terms of the major species $[O_2]$, $[H_2]$ and $[H_2O]$. In model 3 only the expression for [O] was used:

$$[O] = \frac{k_{15}k_{16}}{k_{-15}k_{-16}}\frac{[O_2][H_2]}{[H_2O]} \tag{18}$$

This expression was inserted in Eq. (8) to derive $d[NO]/dt$.

Model 4 The full implications of the partial equilibrium hypothesis of reactions (15), (16) and (17) were considered in model 4. Hence, besides expression (18), the following

relations also result from the partial equilibrium hypothesis:

$$[H] = \left(\frac{k_{15}^2 k_{16} k_{17}}{k_{15}^2 k_{-16} k_{-17}} \frac{[O_2][H_2]^3}{[H_2O]^2} \right)^{1/2} \tag{19}$$

$$[OH] = \left(\frac{k_{16} k_{17}}{k_{-16} k_{-17}} [O_2][H_2] \right)^{1/2} \tag{20}$$

Expression (4) was used to calculate $d[NO]/dt$ together with relations (18), (19) and (20).

Calculation of Source Term of NO Transport Equation

The instantaneous source term of the NO mass fraction transport equation, accounting only for thermal NO, is given by:

$$S_{NO} = M_{NO} \frac{d[NO]}{dt} \tag{21}$$

The Reynolds-averaged source term is computed as:

$$\bar{S}_{NO} = \bar{\rho} \int_0^1 \frac{S_{NO}}{\rho} p(f)\, df \tag{22}$$

where $p(f)$ is the probability density function. The temperature, the density and the chemical species concentrations are expressed as a function of mixture fraction when evaluating the integral in this equation.

Fuel-NO Formation Model

Fundamentals It is assumed that HCN is the only intermediate in the formation of fuel-NO. NO is formed by oxidation of HCN and reduced competitively by reaction of NO with HCN. The reaction rates of these two competitive parallel reactions were determined by De Soete (1975):

$$w_1 = 10^{10} \rho X_{HCN} X_{O_2}^b \exp(-67000/RT) \tag{23}$$

$$w_2 = 3 \times 10^{12} \rho X_{HCN} X_{NO} \exp(-60000/RT) \tag{24}$$

where ρ is the gas density, X is the mole fraction of a species and b is the order of reaction. The order is a function of oxygen concentration and it was also determined by De Soete. Hence, when both thermal and fuel-NO are taken into account, the instantaneous source term of the NO mass fraction transport equation is calculated as:

$$S_{NO} = M_{NO} \frac{d[NO]}{dt} + w_1 - w_2 \tag{25}$$

where M_{NO} is the molar weight of NO. Equation (22) still holds.

The problem of calculation of fuel-NO formation from spray combustion in oil-fired furnaces has been addressed by Hampartsoumian *et al.* (1991). They assume that the nitrogen contained in the fuel enters the flame at a rate proportional to the rate of

droplet evaporation and it is in turn fully converted to HCN. A similar idea underlies the modelling of fuel-NO formation in coal combustion. In this case, the release of fuel nitrogen from the coal is assumed to occur at a rate proportional to volatiles release rate. The volatile nitrogen is assumed to be instantaneously converted to HCN (see, e.g., Smooth and Smith, 1985). Here, we have used three different approaches to model fuel-NO formation.

Model 1 This model solves only a transport equation for NO mass fraction and prescribes the mole fraction of HCN, X_{HCN}, in each control volume. It assumes that X_{HCN} in a control volume is obtained by multiplying the fuel mole fraction in that control volume by the nitrogen content of the fuel. In other words, it is assumed that the nitrogen contained in the fuel is completely released and converted to NO in each control volume. This model fails to account for the transport of fuel and HCN. Therefore, it is expected that it overestimates the fuel-NO concentration.

Model 2 Model 2 solves transport equations for HCN and NO mass fractions. It is assumed that the nitrogen content of the fuel is completely released and converted to HCN at the burners inlet. This assumption is similar to the one of Hampartsoumian *et al.* (1993), since we have assumed that the fuel vaporizes instantaneously. There is no formation of HCN within the boiler but only consumption due to reaction of HCN with O_2 and NO. The instantaneous source term of the HCN mass fraction transport equation is calculated as:

$$S_{HCN} = -w_1 - w_2 \tag{26}$$

and the mean source term is computed from Eq. (22) using S_{HCN} instead of S_{NO}.

Model 3 In this case it is assumed that the source of HCN in each control volume is proportional to the amount of fuel burnt in that control volume. The proportionality constant, λ, is the fuel nitrogen content. Since the combustion model employed here does not require the solution of a transport equation for fuel mass fraction, the amount of fuel burnt in each control volume is not known. However, it can be easily computed from the discretized transport equation for fuel mass fraction using the velocity, fuel mass fraction, density and turbulent viscosity fields calculated by the mathematical model:

$$\bar{S}_{fu} = \frac{\partial}{\partial x_j}(\bar{\rho}\tilde{u}_j\tilde{m}_{fu}) - \frac{\partial}{\partial x_j}\left(\Gamma_{m_{fu}}\frac{\partial \tilde{m}_{fu}}{\partial x_j}\right) \tag{27}$$

In this equation $\Gamma_{m_{fu}}$ is the diffusion coefficient; $\tilde{m}_{fu}$, is the Favre-averaged fuel mass fraction; x_j is the coordinate along j direction; and $\tilde{u}_j$ is the correspondent Favre-averaged velocity component. The instantaneous source of HCN is given by:

$$S_{HCN} = \lambda S_{fu} - w_1 - w_2 \tag{28}$$

The mean source term is calculated as in model 2.

RESULTS AND DISCUSSION

The Studied Boiler

The model was applied to a fuel-oil fired boiler of the Portuguese Electricity Utility. The boiler is fired from 12 burners placed at the front wall in three levels of four burners. The overall dimensions of the combustion chamber are $8.57 \times 11.57 \times 19.96\,m^3$ and it delivers 771 ton/h of steam at 167 bar and 545°C (250 MWe). For modelling purposes only one half of the boiler was studied with symmetry boundary conditions prescribed at the symmetry plane. It was assumed that the fuel vaporizes instantaneously. A mesh with $16 \times 34 \times 60$ grid nodes was used to calculate the reactive flow and a coarser mesh, comprising $10 \times 9 \times 20$ control volumes, was employed to calculate the radiative heat transfer. Grid dependence tests performed in previous studies of this boiler have shown that using these meshes grid dependent effects are negligible.

Thermal NO

Figure 1 shows several profiles of thermal NO mole fraction, on a dry basis, calculated using the 4 variants of the model described in the previous section. These profiles are located in a horizontal plane crossing the axes of the burners at the lower level.

The mole fraction of thermal NO increases along the axis of the burner close to the side wall, i.e., along x direction (see Fig. 1a, $y = 2.43\,m$). Model 1, which assumes equilibrium between oxygen atoms and oxygen molecules, yields predicted NO mole

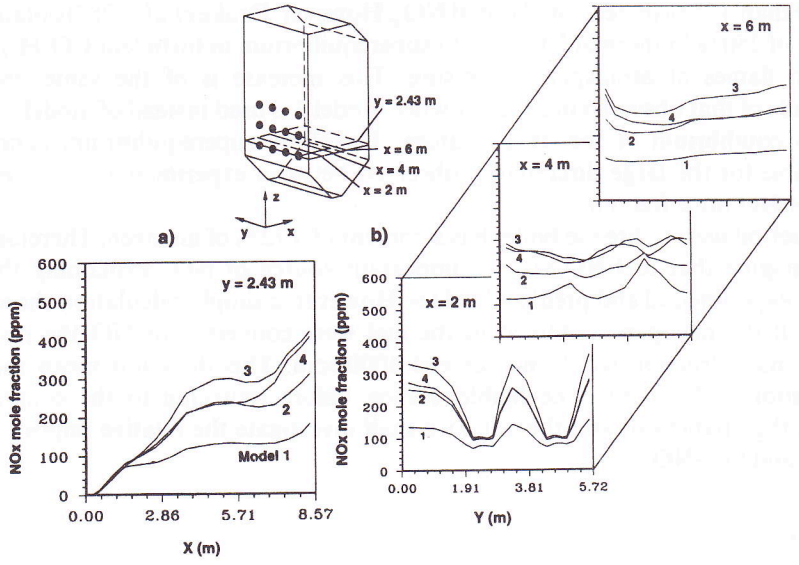

FIGURE 1 Predicted profiles of thermal NO mole fraction through a horizontal plane at the lower burners level.

fractions much smaller than the other models. The assumption of partial equilibrium of reactions (12) and (13) to compute the O-atom concentration (model 2) yields NO mole fractions about 100% higher than those calculated using model 1, except in the neighbourhood of the burner exit where all the models perform similarly. Higher NO mole fractions are estimated using models 3 and 4 which rely on the assumption of partial equilibrium of reactions (15), (16) and (17). NO mole fraction profiles parallel to the front wall at $x = 2$ m, $x = 4$ m and $x = 6$ m are displayed in Figure 1b). NO mole fraction is small in front of the burners, as revealed by the plot at $x = 2$ m, since most thermal NO is formed at the lean edge of the flame front. As the distance from the front wall increases, the NO mole fraction becomes more uniform due to turbulent diffusion. The relative behaviour of the different models described for the profile along the axis of the burner is also observed in the profiles of Figure 1b).

NO_x measurements through port 1.5, lying in the same horizontal plane and placed at the side wall at a distance of 0.5 m from the back wall, are of the order of 4×10^3 ppm (see Cassiano *et al.*, 1994). These values are very high compared with measurements reported in the literature for other boilers, either natural gas, fuel or coal fired boilers (see, e.g., Breen, 1977; Fiveland *et al.*, 1987; Godridge, 1988; Collin and Göransson, 1991; Zennaro *et al.*, 1991; Kwee, 1991). The values reported rarely exceed 1000 ppm. Similarly, numerical predictions of NO concentration in utility boilers are generally below 1000 ppm (see the studies mentioned in the introduction). The NO mole fractions measured by Cassiano *et al.* are almost one order of magnitude higher than those predicted by the thermal NO formation models.

It is well known that thermal NO formation is strongly dependent on the oxygen atom concentration. Superequilibrium concentration of this radical has often been found in different kinds of flames and combustion equipment (see, e.g., Drake *et al.*, 1987). According to Peters and Donnerhack (1981) superequilibrium can account for no more than a 25% increase in thermal NO_x. However, Drake *et al.* (1987) obtained an increase of 250% in thermal NO_x due to superequilibrium in turbulent $CO/H_2/N_2$ jet diffusion flames at atmospheric pressure. This increase is of the same order of magnitude of that observed in Figure 1 when model 3 is used instead of model 1 which assumes equilibrium of the oxygen atom. Therefore, superequilibrium cannot be responsible for the large discrepancy observed between experimental and predicted values of NO mole fraction.

The fuel-oil used to fire the boiler has a content of 0.72% of nitrogen. Therefore, one could imagine that fuel-NO was an important source of NO_x explaining the gap between experimental and predicted values. However, a simple calculation shows that even if all the nitrogen contained in the fuel were converted to NO the resultant fuel-NO mole fraction would not exceed 1000 ppm. This does not mean that the contribution of fuel-NO is negligible. Hence, before returning to the comparison between the predictions and the data, we shall investigate the relative importance of thermal and fuel-NO.

Fuel-NO

Figure 2 shows the predictions of NO mole fraction accounting simultaneously for the thermal and fuel-NO routes for NO formation. The profiles presented are the same

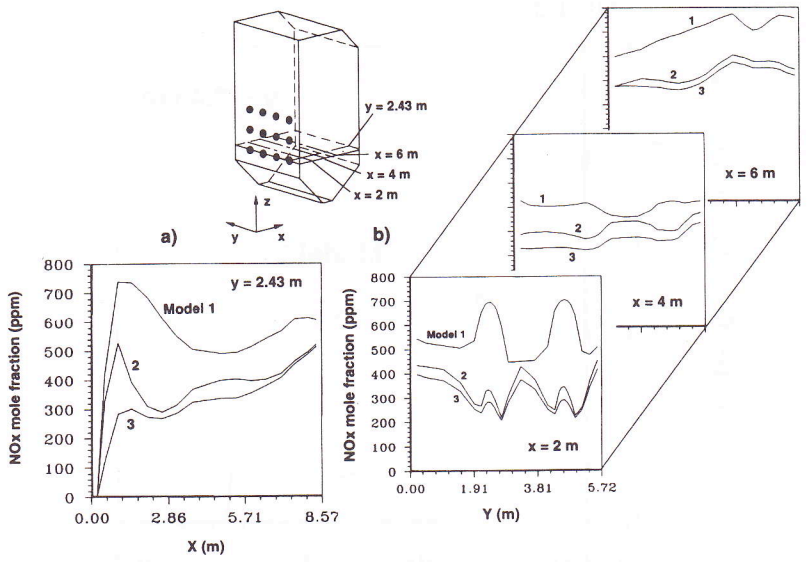

FIGURE 2 Predicted profiles of NO mole fraction (thermal NO plus fuel NO) through a horizontal plane at the lower burners level.

shown in Figure 1. Model 3 of thermal NO formation was used here, as well as in all the following calculations, because it yields higher NO concentrations which are, therefore, closer to measurements.

Model 1 of fuel-NO formation yields the highest NO mole fractions. This is not surprising since, as stated previously, it is expected that this model overestimates NO mole fraction. Model 2 also shows a very steep increase in NO mole fraction close to the burner. However, the predictions obtained using models 2 and 3 are similar elsewhere, although model 2 predictions are slightly higher than those of model 3.

Figure 2a shows that fuel-NO has a significant contribution near the burner exit but its importance decreases farther downstream. However, even considering model 3, which yields the lower NO mole fractions, the contribution of fuel-NO to the total NO formed is at least 20%, as revealed by comparing Figures 1 and 2. In front of the burners, near the front wall, most of the NO is formed from the fuel-NO route.

Further insight into the fuel-NO formation models can be gained by examining the HCN mole fraction profiles displayed in Figure 3. They show that both models 1 and 2 yield very high HCN mole fractions near the burner exit. The order of magnitude of HCN mole fraction calculated using model 3 seems to be more realistic and, therefore, we believe that model 3 should be preferred. It was used in the following calculations.

The contours of NO mole fraction plotted in Figure 4 provide a more general picture of the NO distribution and illustrate the role of thermal and fuel-NO. The vertical plots are normal to the front wall and cross the axes of ther burners close to the side wall. The horizontal plots cross the axes of the burners at the lower level. It can be seen that thermal NO concentration increases from the front to the back wall with relatively uniform values in the ash hopper region. When fuel-NO formation is taken into

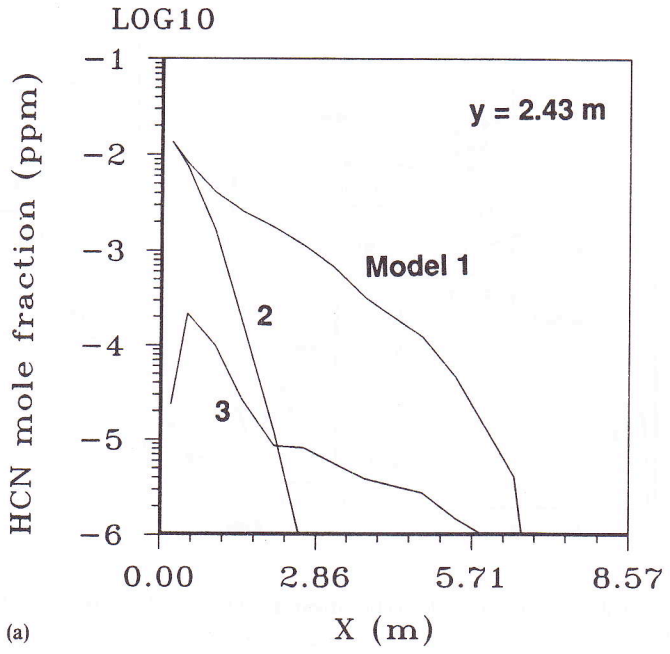

(a)

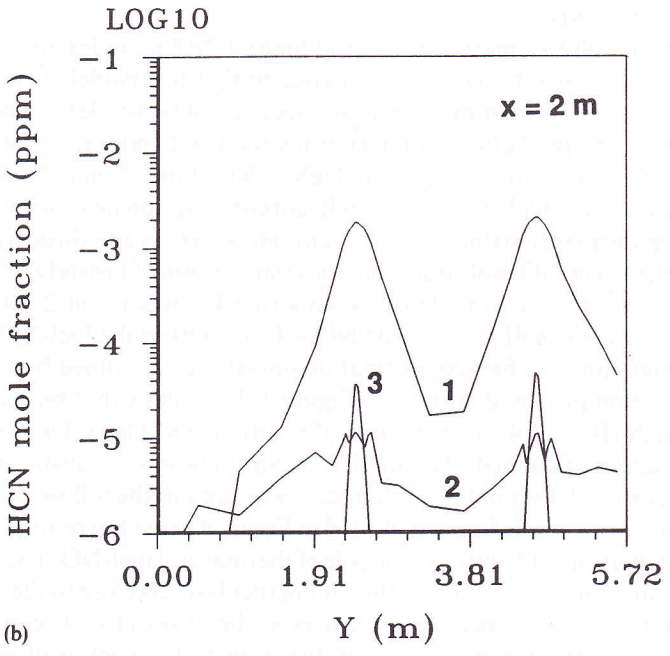

(b)

FIGURE 3 Predicted profiles of HCN through a horizontal plane at the lower burners level.

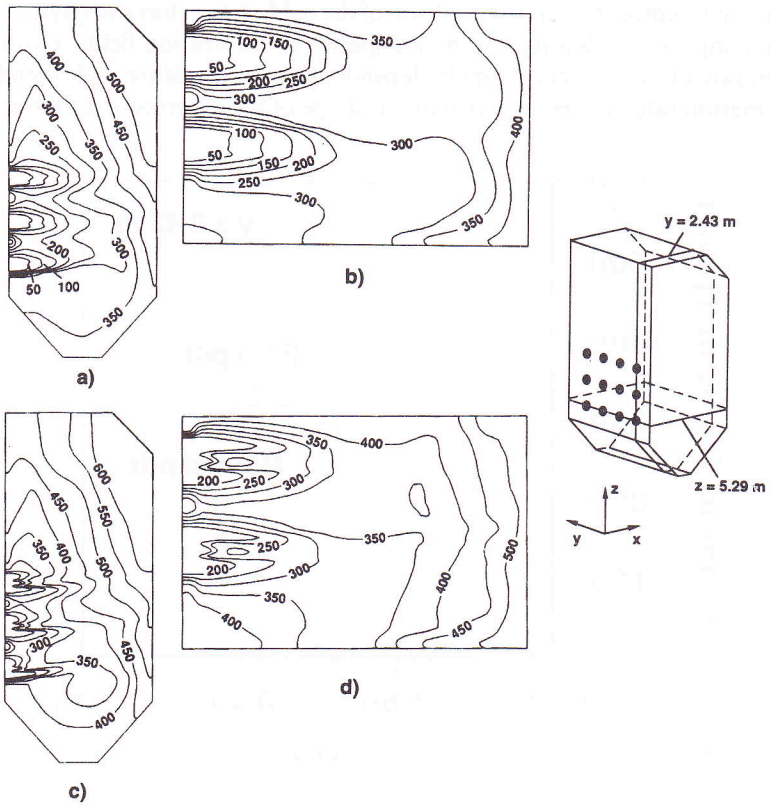

FIGURE 4 Predicted contours of NO mole fraction. (a) Thermal NO, $y = 2.43$ m. (b) Thermal NO, $z = 5.29$ m. (c) Thermal NO plus fuel NO, $y = 2.43$ m. (d) Thermal NO plus fuel NO, $z = 5.29$ m.

account the distribution near the burners is rather different because fuel-NO is formed within the flame zone, with HCN acting as the intermediate species, whereas thermal NO is formed in the post-flame region at the lean edge of the flame front. Elsewhere, both distributions, either neglecting or accounting for fuel-NO, are qualitatively similar. At the combustion chamber exit about 100 ppm are due to the fuel-NO formation.

Comparison Between Predictions and Measurements

The results presented so far show that fuel-NO formation plays an important role but, even though, the levels of predicted NO are significantly lower than the measurements reported by Cassiano *et al.* (1994) which are of the order of 4000 ppm at the burners levels and around 2500 ppm at the boiler nose. It has been shown that the shortcomings of the NO formation models cannot explain the high values measured. Apart from the experimental uncertainties, two other factors might explain the discrepancy: the assumed p.d.f. and errors in the prediction of temperature and species concentration fields. These two factors are analysed below.

It is widely accepted that the precise form of the p.d.f. chosen has a negligible effect on the mean temperature, density and major species concentration fields. However, the formation rate of NO is very strongly dependent on temperature and, therefore, the mean formation rate may be sensitive to the shape of the assumed p.d.f. (Jones, 1979).

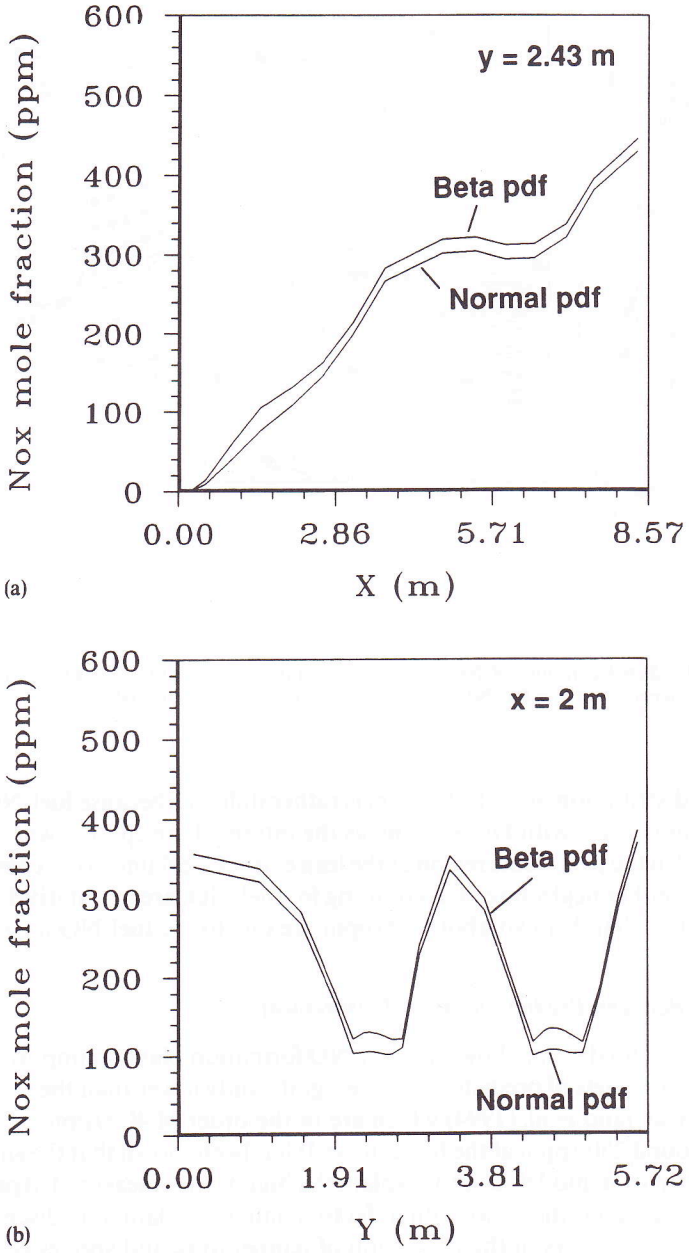

FIGURE 5 Influence of the p.d.f. on the NO mole fraction predictions.

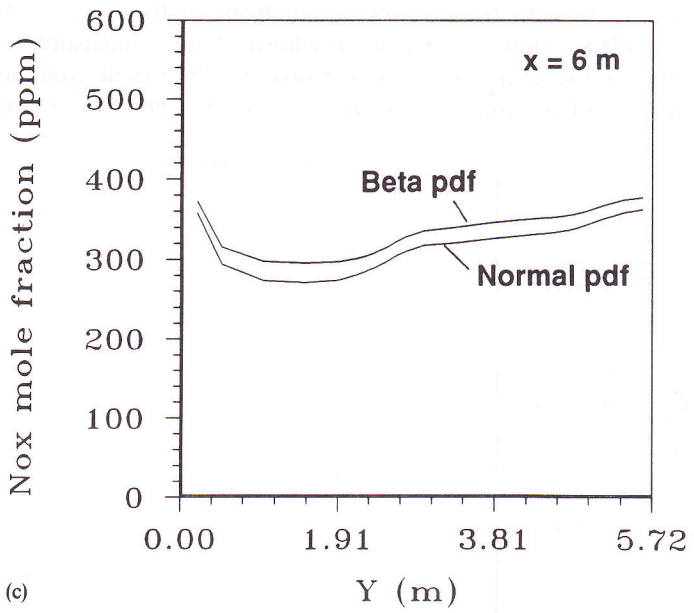

FIGURE 5 *(Continued).*

This was investigated by repeating the calculations using model 3 of thermal NO formation and the beta p.d.f. The results displayed in Figure 5 show that the NO mole fraction is only marginally influenced by the shape of the assumed p.d.f. and that the beta p.d.f. yields slightly higher NO mole fractions than the clipped gaussian p.d.f.

Predicted and measured profiles of temperature, O_2, CO_2, CO and NO mole fractions through inspection ports located at the side walls are presented in Figures 6, 7, and 8.

Port 1.5 is located at the side wall at a distance of 0.5 m from the back wall and at the lower level of burners. The temperature through this port (see Fig. 6a) was underpredicted by 100 to 150 °C. The temperature underestimation is consistent with the underprediction of NO concentration. The mole fractions of O_2, CO and CO_2 are in good agreement with the data (see Fig. 6b). The experimental and measured NO profiles, normalized by the maximum experimental and measured NO mole fractions along that profile, are shown in Figure 6c. It can be seen that the predicted level is almost uniform along this port with a slight decrease near the side wall. The experimental values are even more uniform.

Figure 7 shows several profiles through inspection ports 2.6 and 3.6, at the side wall and at a distance of 0.5 m from the front wall. The temperature profile presented in Figure 7a lies at the top burners level. The species mole fractions profiles plotted in Figure 7b,7c and 7d are contained in the horizontal plane at the intermediate burners level. The temperature is underpredicted except in front of the combustion air inlet. This may be explained by the simplifications in the geometry and the modelling assumptions. The species profiles are in satisfactory agreement with the data. There is an overprediction of CO and an underestimation of the peak of O_2 mole fraction but the trends are correctly predicted. The normalized NO mole fraction profile is in

qualitative agreement with the data except in front of the burner. However, the computed NO mole fractions are significantly lower than the measured ones.

At the boiler nose level and close to the nose the NO mole fraction through a port at the side wall is almost uniform (see Fig. 8). Therefore, there is a good

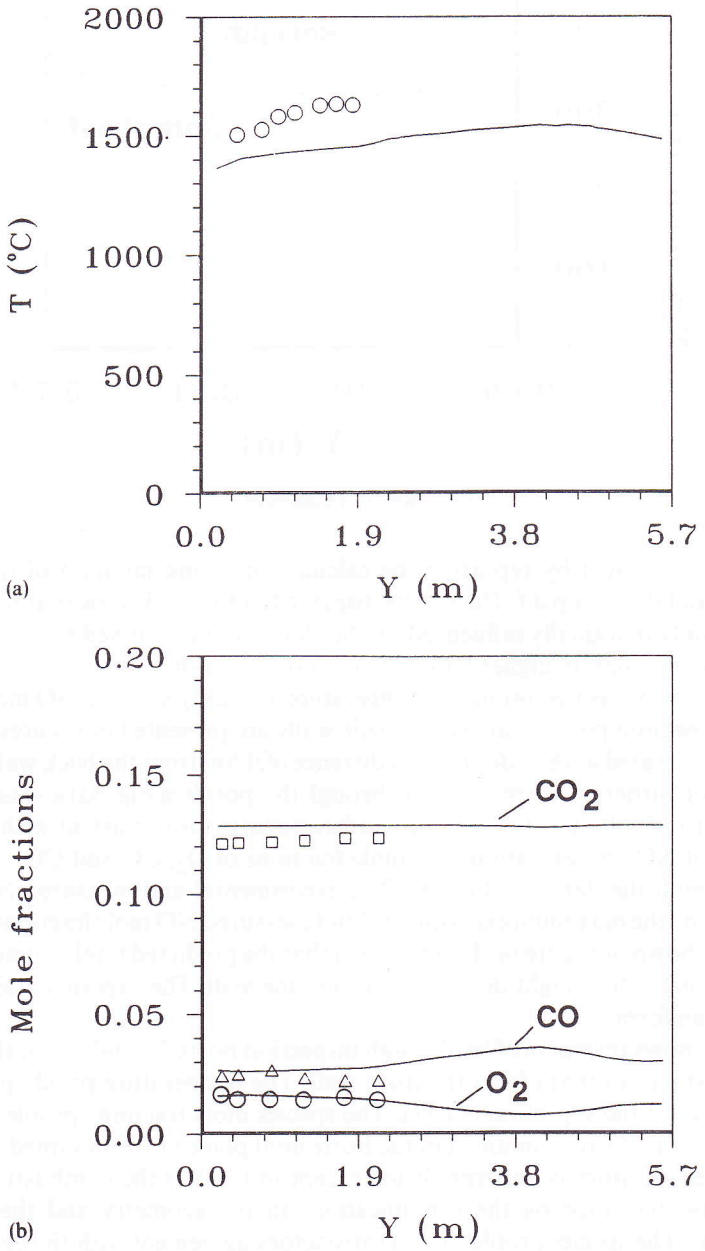

FIGURE 6 Comparison between predictions (solid lines) and measurements (symbols) through port 1.5 (a) Temperature, K. (b) O_2, CO_2 and CO mole fractions. (c) Normalized NO mole fraction.

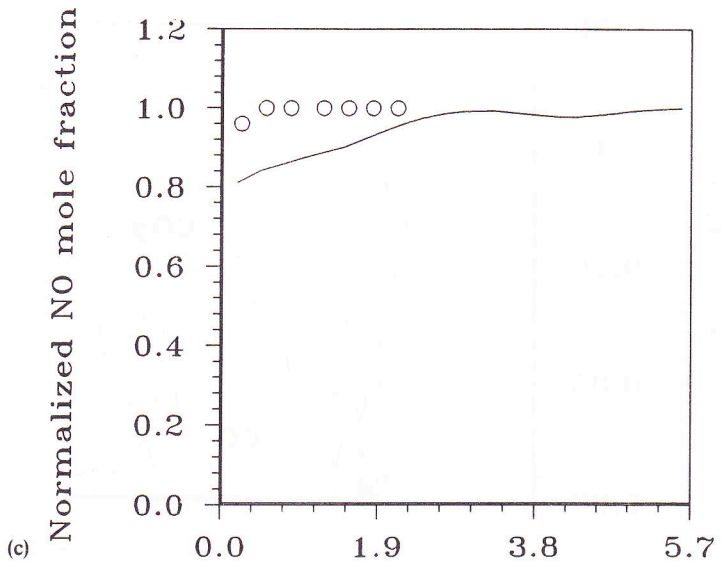

FIGURE 6 *(Continued).*

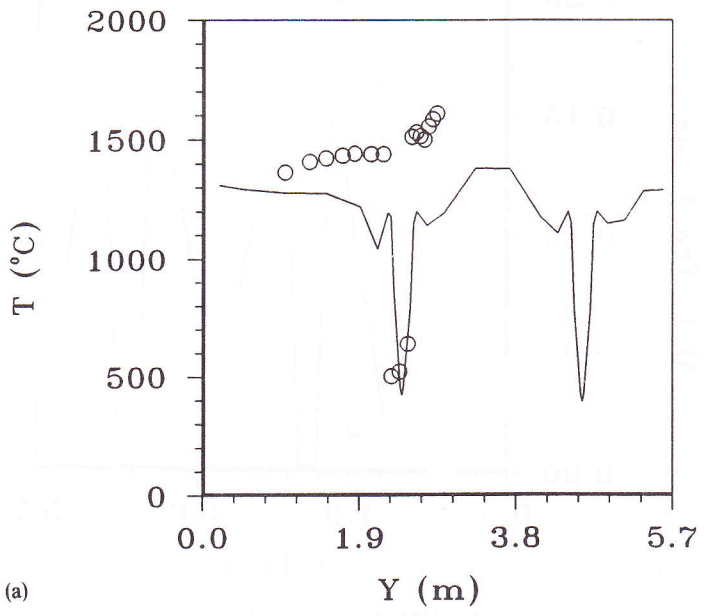

FIGURE 7 Comparison between predictions (solid lines) and measurements (symbols) through ports 2.6 and 3.6. (a) Temperature, K. (b) CO_2 and CO mole fractions. (c) O_2 mole fractions. (d) Normalized NO mole fraction.

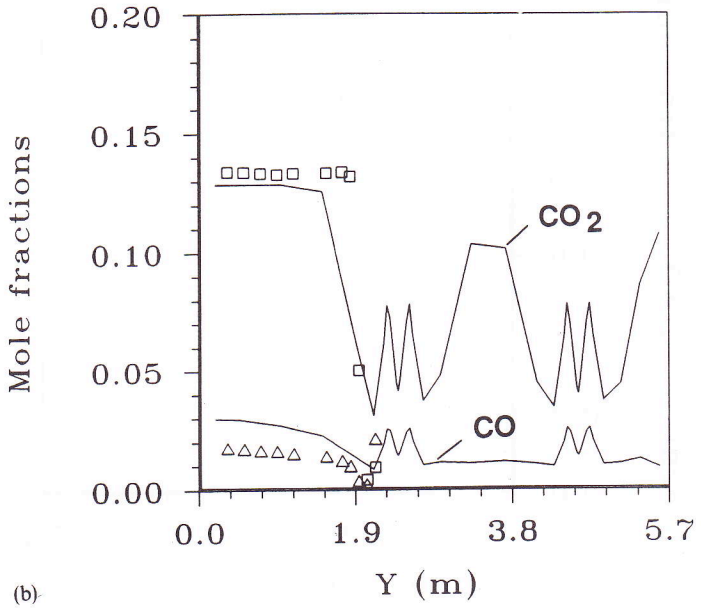

(b)

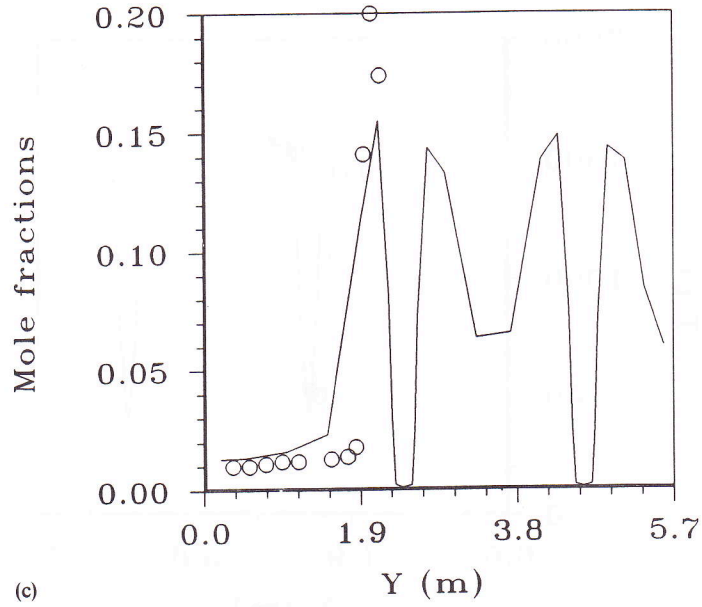

(c)

FIGURE 7 *(Continued).*

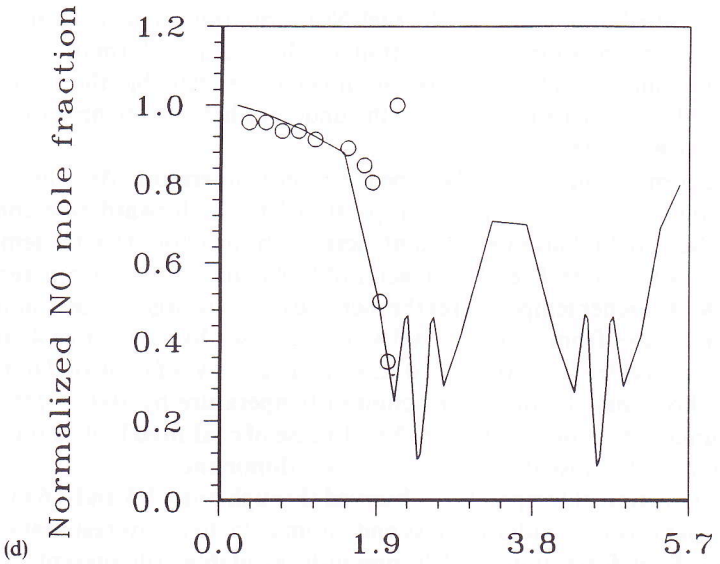

(d)

FIGURE 7 *(Continued).*

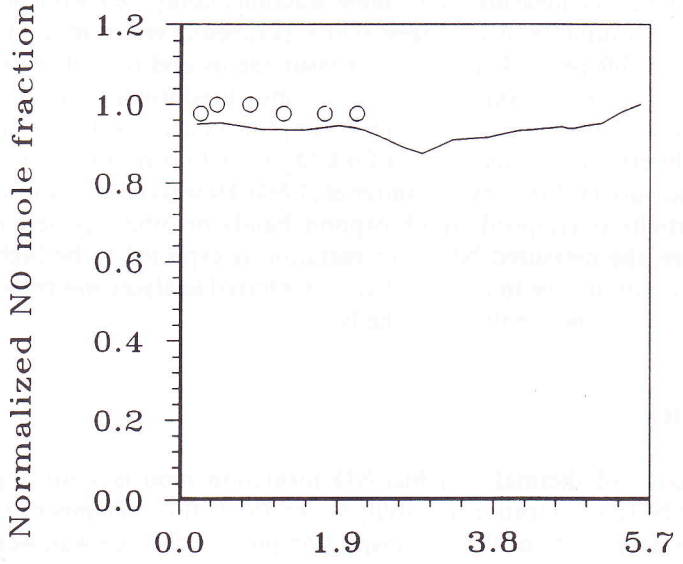

FIGURE 8 Comparison between predicted (solid lines) and measured (symbols) normalized NO mole fraction at the nose level.

agreement between the computed and measured normalized NO mole fraction profiles.

The analysis carried out shows that the predicted NO mole fractions are significantly smaller than the measured values, although there is a good qualitative agreement.

This cannot be attributed either to the fuel-NO formation or to the role of superequilibrium of oxygen atom concentration in thermal-NO formation. Since the influence of the assumed p.d.f. shape was also shown to be negligible, the most probable reasons for the discrepancies observed are the underprediction of temperature and the experimental uncertainties.

The NO concentration is strongly dependent on temperature. As a first approximation, the source of thermal NO is proportional to the forward rate constant of reaction 1, k_1 (see Eq. 9). This rate constant increases by a factor of 6 if the temperature increases from 1400 to 1500 K and by a factor of 13.8 if the temperature increases from 1400 to 1550 K. At higher temperatures the increase is not so large. As an example, if the temperature increases from 1600 to 1700 K, k_1 increases by a factor of 4, and if the temperature increase from 1600 to 1750 K, k_1 increases by a factor of 7.6. However, these figures show that the underprediction of temperature by 100 to 150°C yields a significant underestimation of thermal NO. In case of coal-fired boilers this problem is not so important because the role of fuel-NO is dominant.

The underprediction of temperature observed through ports 1.5 and 3.6 may be due to an overprediction of the radiation loss and, ultimately, to an overestimation of soot concentration. Soot formation models presently available still present recognized shortcomings and more research is needed to improve such models. Higher temperatures would yield higher thermal NO formation rates and higher NO mole fractions.

The high levels of measured NO mole fractions compared with measurements acquired in other utility boilers suggest that experimental errors may, at least, partly account for the differences between the measurements and the calculated NO mole fractions. The gas species concentrations were measured using a gas sampling probe connected to dedicated gas analysers by a sampling system. NO_x was analysed with infrared analysers. The estimated error for CO_2 and CO concentration is 10% of the maximum measured value (see Cassiano *et al.*, 1994). However, the absorption bands of NO are partially overlapped by absorption bands of other species, namely CO, and, therefore, the measured NO_x concentration is expected to be higher than the actual concentration. Due to this problem, the infrared analyser was recently replaced by a chemiluminescence analyser for the NO_x.

CONCLUSION

Several variants of thermal and fuel-NO formation models were applied to the prediction of NO concentration in a utility boiler. Predictions of temperature, O_2, CO_2, CO and NO mole fractions through inspection ports at the side wall were compared with measurements. It was shown that the predicted O_2, CO_2, and CO mole fractions are in good agreement with the available data. The temperature was slightly underestimated but it is in qualitative agreement with the measurements. The fuel-NO formation rate has an important contribution to the total NO formed. The NO mole fraction, however, is significantly underpredicted. It was shown that the role of fuel-NO and the superequilibrium of oxygen atom concentration are not responsible for the differences observed. The most probable reasons for the discrepancies were attributed to the errors in the temperature prediction and in the measurements.

REFERENCES

Abbas, A. S. and Lockwood, F. C. (1986). Prediction of Power Station Combustors, 21st Symp. (Int.) on Combustion, The Combustion Institute, pp. 285–292.

Boardman, R. D. (1990). Development and Evaluation of a Combined Thermal and Fuel Nitric Oxide Predictive Model. Ph.D. Thesis, Brigham Young University.

Bonvini, M., Piana, C. and Vigevano, L. (1991). Predictions of Thermal NO_x Emissions from Utility Boiler Furnaces. Proc. 1st Int. Conf. Combustion Technologies for a Clean Environment, Vilamoura, Portugal, paper 23–3.

Boyd, R. K. and Kent, J. H. (1986). Three-Dimensional Furnace Computer Modelling, 21st Symp. (Int.) on Combustion, The Combustion Institute, pp. 265–274.

Breen, B. P. (1977). Combustion in Large Boilers: Design and Operating Effects on Efficiency and Emissions. 16th Symp. (Int.) on Combustion, The Combustion Institute, pp. 19–35.

Carvalho, M. G. and Coelho, P. J. (1990). Numerical Prediction of an Oil-fired Water-tube Boiler, *Engineering Computations* **7**, 227–234.

Carvalho, M. G., Coelho, P. J. and Costa, F. (1991). Mathematical Modelling of a Power Station Boiler of the Portuguese Electricity Utility, Proc. 2nd European Conf. on Industrial Furnaces and Boilers, Vilamoura, Portugal.

Carvalho, M. G., Durão, D. and Pereira, J. (1987). Prediction of the Flow, Reaction and Heat Transfer in an Oxy-fuel Furnace. *Engineering Computations*, **4**, 23–34.

Cassiano, J., Heitor, M. V., Moreira, A. L. and Silva, T. F. (1994). Temperature, Species and Heat Transfer Characteristics of a 250 MWe Utility Boiler. *Combust. Sci. Tech.*, **98**, 199–215.

Coimbra, C., Azevedo, J. and Carvalho, M. G. (1993). 3-D Numerical Model for Predicting NO_x Emissions from a Pulverized Coal Industrial Combustor. *Fuel*, **73**, 1128–1134.

Collin, R. and Göransson, O. (1991). Reburning – modelling and Experiments in a 125 MW Boiler. Proc. 2nd European Conf. Industrial Furnaces and Boilers, Vilamoura, Portugal.

De Michele, G., Pasini, S. and Tozzi, A. (1991). Simulation of Heat Transfer and Combustion in Gas- and Oil-fired Furnaces. Proc. 2nd European Conf. Industrial Furnaces and Boilers, Vilamoura, Portugal.

De Soete (1975). Overall Reaction Rates of NO and N_2 Formation from Fuel Nitrogen. 15th Symp. (Int.) on Combustion, The Combustion Institute, pp. 1093–1102.

Drake, M. C. Correa, S. M., Pitz, R. W., Shyy, W. and Fenimore, C. P. (1987). Superequilibrium and Thermal Nitric Oxide Formation in Turbulent Diffusion Flames. *Combustion and Flame*, **69**, 347–365.

Dupont, V., Pourkashanian, M. and Williams, A. (1993). Modelling of Process Heaters Fired by Natural Gas. *J. Institute of Energy*, **66**, 20–28.

Epple, B. and Schnell, U. (1992). Modelling and Simulation of Coal Combustion Process in Utility Boiler Furnaces. Proc. 2nd Int. Forum Expert Systems and Computer Simulation in Energy Engineering, Erlangen, Germany, paper 12-L.

Fiveland, W. A. and Wessel, R. A. (1988). Numerical Model for Predicting Performance of Three-dimensional Pulverized-fuel Fired Furnaces, *ASME J. Eng. Gas Turbines and Power*, **110**, 117–126.

Fiveland, W. A. and Wessel, R. A. (1991). Model for Predicting the Formation and Reduction of Nitric Oxide Pollutants in Three-dimensional Furnaces Burning Pulverised Fuel. *J. Institute of Energy*, **64**, 41–54.

Fiveland, W. A., Wessel, R. A. and Eskinazi, D. (1987). Pollutant Model for Predicting Formation and Reduction of Nitric Oxides in Three-dimensional, Pulverized Fuel-fired Furnaces. 24th National Heat Transfer Conference, Pittsburgh, pp. 39–49.

Godridge, A. M. (1988). Flue Gas Recirculation in Oil-fired Plant. *J. Institute of Energy*, **61**, 38–54.

Görner, K. and Zinser, W. (1988). Prediction of Three-dimensional Flows in Utility Boiler Furnaces and Comparison with Experiments, *Combust. Sci. Tech.*, **58**, 43–58.

Hampartsoumian, E., Nimmo, M., Pourkashanian, M., Williams, A. and Missaghi, W. (1993). The Prediction of NO_x Emissions from Spray Combustion. *Combust. Sci. Tech.* **93**, 153–172.

Iverach, D., Basden K. S. and Kirov, N. Y. (1973). Formation of Nitric Oxide in Fuel-lean and Fuel-rich Flames, 14th Symp. (Int.) on Combustion, The Combustion Institute, pp. 767–775.

Jones, W. P. (1979). Model for Turbulent Flows with Variable Density and Combustion. Von Karman Institute for Fluid Dynamics, Lecture Series 1979-2.

Kwee, H. K. (1991). Experiences with the New Developments in Advanced Low-NO_x Combustion of Fossil Fuels for Industrial and Utility Boilers. Proc. 1st Int. Conf. Combustion Technologies for a Clean Environment, Vilamoura, Portugal, paper 16.1.

Peters, N. and Donnerhack, S. (1981). Structure and Similarity of Nitric Oxide Production in Turbulent Diffusion Flames. 18th Symp. (Int.) on Combustion, The Combustion Institute, pp. 33–42.

Robinson, G. F. (1985). A Three-dimensonal Model of a Large Tangentially Fired Furnace, *J. Institute of Energy*, **58**, 116–150.

Schott, G. L. (1960). Kinetic Studies of Hydroxyl Radicals in Shock Waves III. The OH Concentration Maximum in Hydrogen-Oxygen Reaction. *J. Chemical Physics*, **32**, 710.

Smoot, L. D. and Smith, P. J. (1985). *Coal Combustion and Gasification*, Plenum Press, New York.

Warnatz, J. (1992). Chemical Kinetics for Combustion. Von Karman Institute for Fluid Dynamics. Lecture Series 1992-03.

Zennaro, A., Piantanida, A., Benanti, A., De Michele, G. and Tarli, R. (1991). Low NO_x Combustion Modifications on Italian Utility Boilers. Proc. 1st Conf. Combustion Technologies for a Clean Environment, Vilamoura, Portugal, paper 2.5.